Advanced Steel Construction – Vol. 18 No. 4 (2022) 753–762
DOI:10.18057/IJASC.2022.18.4.3

BOND-SLIP TESTING AND PERFORMANCE EVALUATION OF SEMI-RIGID FLANGE FOLDED WEB SHEAR KEYS

Zhen-Shan Wang [1, 2, *], Hua-Qian Qin [2], Yong Yang [2], Yun-He Liu [1], Hong-Chao Guo [2] and Jian-Bo Tian [2]

[1] *State Key Laboratory of Eco-hydraulics in Northwest Arid Region of China, Xi'an University of Technology, Xi'an 710048, China*
[2] *School of Civil Engineering and Architecture, Xi'an University of Technology, Xi'an 710048, China*
** (Corresponding author: E-mail: wangdayuwang@126.com)*

ABSTRACT

The shear key is crucial to the overall mechanical performance of the structure. A new type of semi-rigid connector-flange folded web shear key was proposed to determine the effective unity of higher bearing capacity and deformation. A total of five groups of specimens were designed, and the push-out test method was used to evaluate the ultimate bearing capacity, bond-slip process, failure mode, and strain distribution of the new shear key. The results show that before sliding, the embedded effect of the concrete and shear key is significant, and it has a significant sliding stiffness. After sliding, the steel plate in the middle of the opening of the outer folded plate buckles, which shows certain semi-rigid characteristics. Compared with equal-area studs, the bearing capacity of the new shear key is increased by more than 40%, and the deformation capacity exceeds 60 %, indicating good bond-slip performance. The constraint range of the shear key is greatly improved compared with the stud, and a trapezoidal area of constraint centered on the shear key is formed, accounting for more than half of the area of the concrete slab. Based on an experimental study, a practical calculation method of ultimate bearing capacity of the shear key is proposed, which can meet engineering safety requirements. Based on the analysis of bond-slip characteristics of different forms of shear keys, compared with the rigid T-shaped shear key, the slip load and ultimate bearing capacity of the new shear key are found to be increased by 39 % and 74 %, respectively, and the deformation capacity is increased more than 10-fold. Compared with the flexible stud shear connectors, the sliding load is increased by 86 %, the ultimate bearing capacity is increased more two-fold, and the stiffness is increased by nearly five times. The device exhibits good comprehensive performance.

ARTICLE HISTORY

Received: 9 July 2021
Revised: 16 April 2022
Accepted: 2 May 2022

KEYWORDS

Semi-rigid shear key;
Bond slip;
Mode of failure;
Ultimate bearing capacity;
Design approach

1. Introduction

Steel-concrete composite beam-slab structure can give full play to the mechanical properties of steel and concrete, forming complementary advantages, and is increasingly widely applied in structural engineering. The composite structure connects the two materials using shear connectors, and makes them work together through friction, mechanical bite force, and bonding force. As an important component of steel-concrete composite beam and slab, shear connectors have two main functions: resisting horizontal shear force and ensuring cooperative action between steel and concrete, and resisting the upward lift at the interface between steel beam and concrete. There are various forms of shear connectors, and their performance differences are also significant. At present, they are mainly divided into two categories: rigid and flexible shear connectors. The stiffness of a rigid shear connector is far greater than that of the concrete structure, which can produce strong constraints thereon, and the bond-slip deformation between concrete and steel structure is controlled; however, due to the shear bond stiffness being too large, when the load exceeds the ultimate bearing capacity, resulting in contact with the concrete leading to crushing or shear failure, the structural deformation capacity is poor. The stiffness of the flexible shear connector is relatively small, the concrete slab can slip with it, and the structural deformation ability is better; however, the constraint on the slip deformation of the concrete structure is reduced due to the low stiffness of the shear key itself. Under the action of rare earthquakes, excessive slip deformation will cause some damage to the structure, and the second-order effect is more serious, causing a significant reduction in the overall safety of the structure. To improve the overall performance of steel-concrete composite beam-slab structure, the analysis of new shear connector connection form and mechanical performance is a focus of much of the research into composite structures.

The stud is one of the most common shear connectors used at present. As a typical flexible shear key, it is widely applied in steel-concrete composite beams and slabs. At present, the influences of stud length, diameter, and number on bond-slip performance and stiffness were evaluated by push-out tests and numerical simulation [1-3]. On this basis, the calculation methods of bearing capacity and stiffness were analyzed, and suggestions for engineering design were proposed. Chaves Marina *et al*. [4] evaluated the relationship between the mechanical properties of concrete-filled steel tube and the bolt shear bond. The results show that the best matching value between the thickness of steel tube and the diameter of bolt shear bond ranges between 1.3 and 2. Angular steel shear parts exhibit the characteristics of high bearing capacity and convenient processing. Arévalo [5], Qiu [6], and Jiang [7] studied the shear keys of angle steel to reveal the influences of angle steel size and angle, the bearing capacity, and shear stiffness of angle steel through monotonic and cyclic loading, and proposed practical calculation formulae for strength and stiffness. Rigid shear connectors are also used in practice. Maleki [8] and Yan [9] studied the mechanical properties of groove shear connectors under monotonic and low cycle fatigue loads. The results show that the failure modes are mainly shear failure and concrete failure. Compared with the same monotonic load condition, the strength is reduced by 10% to 20% under repeated loading. Vianna [10], Isabel [11], Huang [12] and Li [13] investigated the flange size and opening size of a T-shaped plate and a T-shaped perforated plate, and demonstrated its failure mode with a focus on its ultimate bearing capacity and ductility. On this basis, they established a formula for calculating the bearing capacity of shear connectors of T-shaped plates and T-shaped perforated plates, which were close to measured experimental values.

As a new type of shear connector, the PBL has been gradually applied in steel-concrete composite bridge structure. Yong Yang, Mohammed, Yang [14], Mohammed [15], and Zhang [16] conducted experimental research into the bearing capacity and failure mode of PBL connector to analyze the failure mechanisms. It is found that this type of shear connector has obvious embedded effects when set in concrete, offering good mechanical performance. Rodrigues [17], Chen [18] and Yang [19,20] evaluated the influences of the number and diameter of holes on the bearing capacity of PBL connectors by push-out tests. The results showed that the number of holes had a significant impact on the bearing capacity of PBL connectors, while the diameter of holes exerted little effect on the bearing capacity of PBL connectors. Weiqing [21] explored the main factors influencing shear capacity of single-hole PBL connectors based on existing experimental and theoretical studies and established a formula for the shear capacity. Costa-Neves [22], Xue [23], Zhang [24], and Wang [25] studied the influences of the reinforcement in the hole on the bearing capacity, ductility, and failure mode of PBL connector through the push-out test. It is found that the reinforcement in the hole can improve the ultimate bearing capacity, and the ultimate bearing capacity increases with the increase in the diameter of the reinforcement, but the ductility of the specimen is poor. Di *et al*. [26] assessed the mechanical properties and bearing mechanism of large-size PBL connectors under strong constraint conditions and found that the ductility of connectors increases with the increase in the size of the hole under strong constraint conditions. Based on an experimental study, Zhao [27] and Shi [28] conducted numerical simulation of shear connectors with openings, mainly focusing on their layout and opening diameter. The results indicated that it is feasible to use ABAQUS to analyze the mechanical properties of PBL connectors. Chen *et al*. [29] studied the shear bearing capacity, stiffness, and deformation capacity of PBL shear keys with straight and inclined plates. They found that the bearing capacity of PBL shear keys with straight and inclined plates was equivalent, but

the PBL shear keys with inclined plates had higher stiffness and better deformation capacity. Ramasamy *et al*. [30] changed the hole shape of the connector to a triangle for test purposes, and the results showed that the slip capacity of the connector with a triangular hole was significantly improved. Li [31] and Suzuki [32] found that the bearing capacity of PBL connectors was reduced by 55% compared with monotonic loading by testing PBL connectors using cyclic loading. Zhang *et al*. [33] proposed an embedded connector with the flange. Through eight groups of push-out tests, it is found that the bearing capacity of the connector is about 1.5 times that of the embedded connector when the flange is stable.

Based on research into traditional connectors, many scholars have studied special-shaped shear connectors with various waveforms. Chen [34], Ruinian [35] and Su [36] found that the deformation of shear connectors with corrugated openings was obvious and the rate of utilization of materials was high by investigating shear connectors with corrugated openings. Sang-Hyo Kim [37-39] studied the mechanical properties of Y-type shear connectors. The results show that the shear strength, shear stiffness, and ductility of Y-type shear connectors are better than those of traditional shear connectors. Nie [40] and Zhuang [41] conducted experimental research on the new type of T-joints with pull-out and non-shear resistance. The results indicated that the joint can improve the mechanical properties in the zone of negative bending moment of the composite beam, and the anti-slip effect is good under low load. Li *et al*. [42] proposed a type of perforated plate connector; through the push-out testing of six groups of specimens, they found that the initial stiffness and bearing capacity of the connector were large. According to the test results, the calculation formula of bearing capacity was established, which was in good agreement with experimental values. Zhao *et al*. [43] proposed a dumbbell-shaped connector for the shortcomings of traditional stud connectors. Through the finite element software for shear analysis, it was found that the dumbbell-shaped connector can significantly improve the shear bearing capacity, and under the same shear effect, the material consumption can be reduced by more than 40 % compared with the use of a stud.

From the current situation, flexible shear key studs are widely used, with good deformation ability and high ability to work together with concrete, but under the action of greater shear force, especially under the condition of strict requirements for slip, rigid shear keys are needed; however, due to the large stiffness of the rigid shear key, the concrete in contact with it is destroyed, and the structural deformation capacity is low. In order to further balance “stiffness” and “deformation”, the concept of a “semi-rigid” shear key is proposed, which can allow a certain deformation while providing large shear capacity, and can meet the dual requirements of “constraint” and “deformation”. Based on the existing research results pertaining to shear connectors, a “flange folded web shear key” is proposed. The design concept entails a web of folded plate form, reducing the web stiffness. Meanwhile, the stiffness of two principal axes of shear keys is balanced to avoid the formation of strong and weak axes. The web opening treatment can improve the embedded effect of shear keys and concrete, which is beneficial to stress transfer and improving structural integrity thereof. By setting the flange, the stability of the web is improved and the anti-lifting effect of shear keys is enhanced.

Herein, five groups of specimens were designed by a push-out test method. The ultimate bearing capacity and failure mode of the shear key were determined to reveal its failure characteristics and constraint effect, and the bond-slip performance and failure mechanism of the shear key were obtained. On this basis, the ultimate bearing capacity and design method were studied. Finally, practical calculation formulae and design suggestions were provided. The bond-slip performance of “new semi-rigid shear key”, “T-rigid shear key”, and a “stud flexible shear key” was compared and evaluated. This paper can provide an experimental basis and technical support for the engineering application of these modified shear keys.

2. Experimental work

2.1. Shear key design

A total of five groups of specimens were designed, and the parameters of each specimen are listed in Table 1. S−1 and S−3 are shear keys of flange double-folded web design, in which steel bars are inserted in the opening of S−3. S-2 and S-4 are shear keys of flange triple-folded web design, in which steel bars are inserted in the opening of S−4. Except for the different forms of folding plates, the material properties, opening size and folding angle of each group of specimens are the same. S-5 is a stud shear connector. The specific dimensions are as follows: taking studs which are widely used in engineering as design reference, the design idea of one shear key equivalent to two studs was adopted (Fig. 1). According to the specification *Cylindrical Head Studs for Arc Stud Welding (GBT10433-2002)* [44], M22 × 90 mm was selected as the stud, and its cross-sectional area was 760 mm^2. The thickness of the folded plate and the upper cover plate of the double-folded plate shear key was 6 mm. The length of the folded plate was 85 mm, and the height was 90 mm. The double-folded plates were at 90° to each other. The length of the upper cover plate was 120 mm, and the middle part of the folded plate was opened with a long round hole of 25 mm in diameter and 70 mm in height to ensure the penetration of concrete. Triple-folded plate shear key on both sides of the folded plate is 63 mm long and the middle folded plate length was 50 mm. The remaining dimensions were consistent with those of the double-folded plate shear key. Through calculation, the areas of the middle section of the double-folded plate and triple-folded plate shear keys are 720 mm^2 and 606 mm^2, respectively (Fig. 2).

Table 1
Specimen parameters

Number and form of shear keys	Inserted rebar	Filling material
S-1 Double-folded plate shear key	NO	C30 commercial concrete
S-2 Triple- folded plate shear key	NO	C30 commercial concrete
S-3 Double-folded plate shear key	YES	C30 commercial concrete
S-4 Triple-folded plate shear key	YES	C30 commercial concrete
S-5 Stud connector	—	C30 commercial concrete

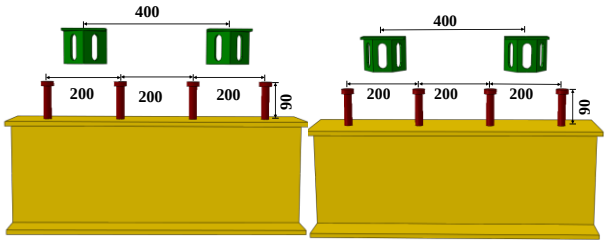

(a) Shear key distribution of flange double-folded web (b) Shear key distribution of flange triple-folded web

Fig. 1 Distribution of shear keys

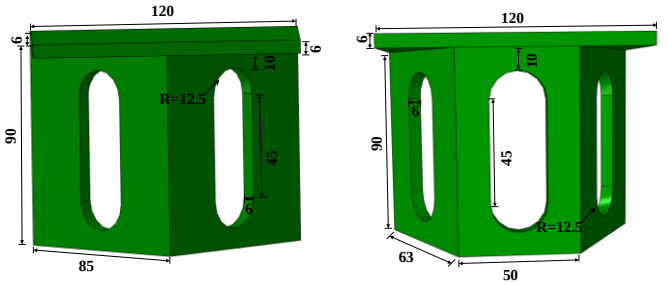

(a) Shear key of flange double-folded web (b) Shear key of flange triple-folded web

Fig. 2 Form and size of shear keys

2.2. Processing and manufacturing of pushout specimens

The pushout specimen composition and reinforcement arrangement are shown in Fig. 3. The concrete slab measured 580 mm × 550 mm × 130 mm, of which 60 mm was prefabricated and 70 mm was cast-*in-situ*. C30 commercial concrete was used, and the joint was also filled with C30 commercial concrete. The steel beam was fabricated in Q235 grade H steel, the specification of which was HW300×200×8×12 (mm), the shear key was made from Q235 B grade steel, the longitudinal reinforcement of concrete slab was of HRB400Φ8-form, and the rebar at the opening is in an HRB400Φ12 arrangement. The steel and concrete used in the test were tested (Tables 2 and 3). The specimens were formed as follows: a 60-mm thick reinforced concrete slab was prefabricated, cued, and assembled on both sides of the steel beam, the longitudinal reinforcement of the slab was thus broken at the joint. This prefabricated plate was used as the bottom template, and the joint at the shear key was filled before the post-cast laminated layer was constructed. The longitudinal reinforcement was arranged as a whole. After binding, the whole casting was formed (Fig. 3d).

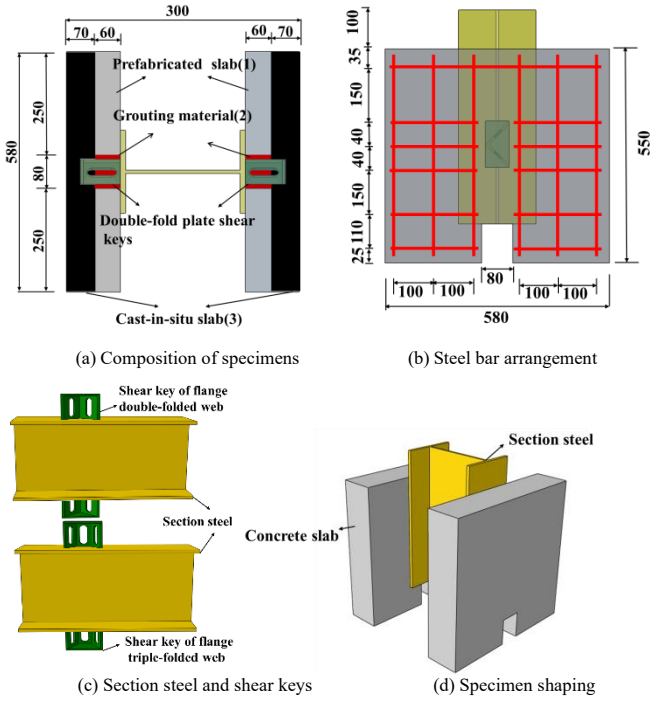

(a) Composition of specimens (b) Steel bar arrangement

(c) Section steel and shear keys (d) Specimen shaping

Fig. 3 Composition and design of the specimen

Table 2
Measured material properties of concrete

Material type	f_{ck} (MPa)	$f_{cu,k}$ (MPa)	f_c (MPa)	E_c (N/mm^2)
Commercial concrete	27	40.35	19.3	33827

NOTE: $f_{cu,k}$: Standard value of concrete cube compressive strength;
f_{ck}: Axial compression strength of concrete;
f_c: of the designed axial compressive strength of concrete;
E_c: Modulus of elasticity of concrete

Table 3
Test results: steel and reinforcement

Specimen number	f_y (MPa)	f_u (MPa)	ε_y (%)	ε_u (%)	E (GPa)
Reinforcement (Φ6)	572	642	0.5	3.15	189
Reinforcement (Φ8)	472	662	0.47	6.33	183
Reinforcement (Φ12)	509	583	0.34	9.9	187
Steel plate	255	410	0.76	9.49	214

NOTE: f_y: Yield strength; f_u: Tensile strength;
ε_y: Yield strain; ε_u: Tensile strain; E: Elastic modulus of steel

2.3. Loading device and programs

The bond-slip performance of the shear key was studied by push-out tests. The specimen was placed on the long column press, steel plate was placed on the top of the steel, and fine sand was laid on the rigid base and steel plate to avoid stress concentration (Fig. 4).

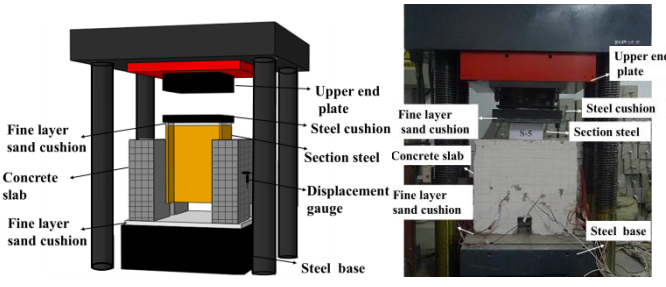

(a) Schematic representation of the loading device (b) Actual loading device

Fig. 4 Test device

The loading scheme adopts load and displacement mixed loading. It first controls force loading, loading to steel beam slip, and then displacement control, until failure (Table 4).

Table 4
Loading scheme

Step	Control mode	Control parameter	Jump options
1	Constant speed force	0.15 kN/s	Before sliding, the force control loading is used, and each loading is 100 kN for two minutes. When the loading is loaded to the specimen sliding, the displacement control is changed.
2	Constant speed displacement	0.03 mm/min	When loading to about 85 % of the ultimate load, stop loading.

3. Experimental results

3.1. Failure process analysis

S-1 is a shear key of flange double-folded web design. At the beginning of loading, there is no obvious failure of the specimen. When the load reaches 210 kN, the steel beam slips, and as the load is increased, small cracks are formed near the shear key (Fig. 5b). With increasing load, the cracks gradually extend and form two main cracks at 45° on both sides of the shear key (Fig. 5b). After reaching the ultimate bearing capacity, multiple inclined cracks are generated around the shear key, resulting in the failure of the concrete slab. The cracks are mainly vertical crack, and the horizontal expansion area is mainly covered by oblique cracks. The maximum horizontal crack range is about two-thirds of the plate width, and the height is about three-fifths of the plate height. The overall crack area is basically trapezoidal (Fig. 5b). When the load is stopped at 80% of the ultimate bearing capacity, the concrete around the shear key is stripped. The failing specimen is shown in Fig. 5c. Along the push-out direction, the overall lateral bending occurs, the outer plate of the folded plate is obviously buckling, and the inner edge of the hole is slightly bent.

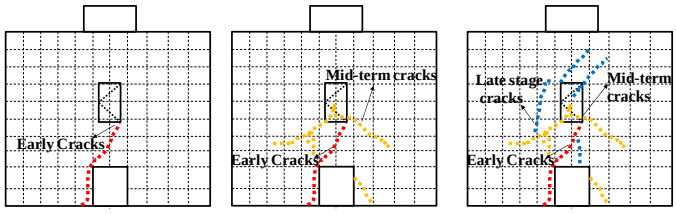

(1) Load: 210 kN (2) Load: 410 kN (3) Displacement: 6 mm

(a) Crack development in Specimen S-1

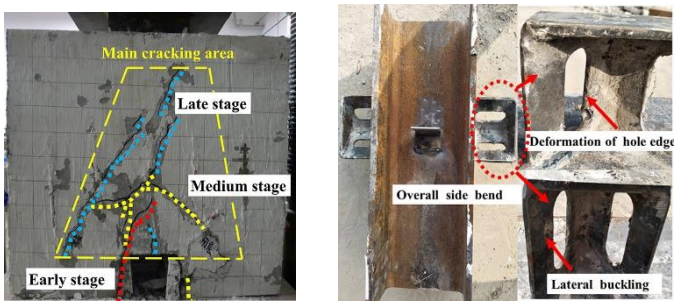

(b) Concrete slab cracks (c) Shear bond damage

Fig. 5 Destruction of Specimen S-1

S-2 is a shear key of flange triple-folded web design; when the load reaches 250 kN, the steel beam begins to slip, and the concrete floor undergoes vertical cracking (Fig. 6b). As the load is increased, the cracks at the bottom of the concrete slab extend upward, and multiple oblique cracks appear (Fig. 6b). After reaching the ultimate load, oblique cracks at 45° to the shear key appear on both sides and at the bottom of the shear key, and the right-hand oblique cracks gradually extend to the bottom of the concrete slab. The maximum crack width is about two-thirds of the slab width, and their height is about four-fifths of the slab height: the overall distribution thereof is trapezoidal (Fig. 6b). Loading to

80% of the ultimate bearing capacity to stop loading, shear bond around the concrete is tripped (Fig. 6c), the web position undergoes bending, along the push-out direction, the lateral buckling of the folded plate is obvious, the edge of the opening suffers little damage, and the middle folded plate remains unbuckled.

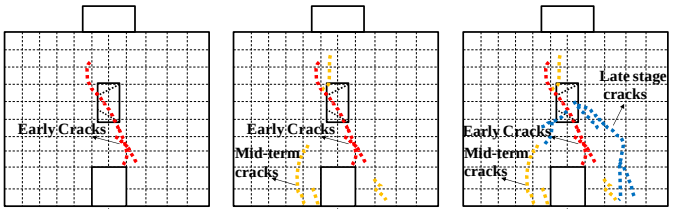

(1) Load: 250 kN (2) Load: 370 kN (3) Displacement: 6 mm

(a) Crack development in Specimen S-2

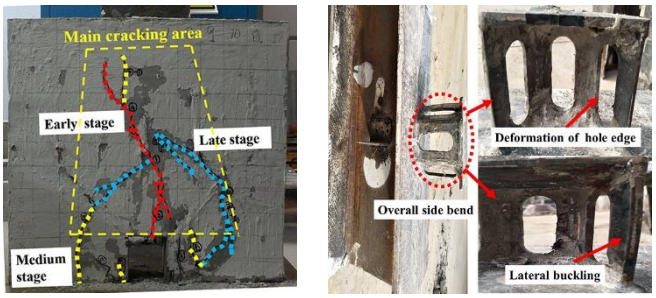

(b) Concrete slab cracks (c) Shear bond damage

Fig. 6 Destruction of Specimen S-2

.

S-3 is a double-folded plate shear key design with rebar inserted in the hole. At a load of 270 kN, the steel beam slips, vertical cracks appear in the middle of the shear key, and oblique cracks appear in the bottom at 45° direction to the base (Fig. 7b). As the load increases, several cracks appear in the middle and bottom of the concrete slab (Fig. 7b). After reaching the ultimate load, a large crack is formed in the vertical direction of the upper part of the shear bond, and the concrete slab is severely damaged. The bottom crack covers the full width of the section, and vertical cracking area reaches three-quarters of the plate height. The crack form is akin to that in other specimens. Vertical cracks are found to run along the shear bond, and oblique cracks are mainly seen elsewhere (Fig. 7b). When the bearing capacity decreases to 80% of the ultimate bearing capacity, the loading is stopped, and the concrete is stripped. The failure of shear keys and reinforcement is shown in Fig. 7c, which is consistent with the failure of Specimen S-1, and the reinforcement is bent.

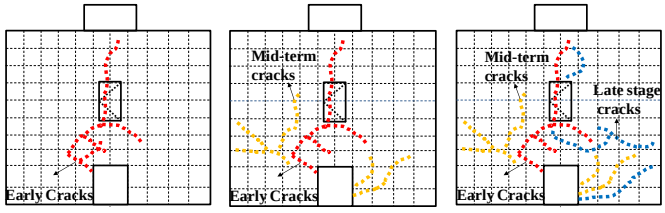

(1) Load: 270 kN (2) Load: 410 kN (3) Displacement: 7 mm

(a) Crack development in Specimen S-3

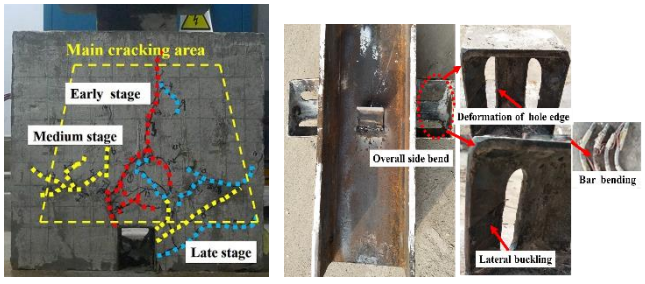

(b) Concrete slab cracks (c) Shear key and steel bar damage

Fig. 7 Destruction of Specimen S-3

S-4 is a triple-folded plate shear key design with rebar inserted in the hole. When the load reaches 270 kN, the steel beam begins to slip, several cracks appear at the bottom of the concrete slab and continue to extend upwards (Fig. 8b). With increasing load, a 45° oblique crack appears near the shear key (Fig. 8b). When reaching the ultimate load, the cracks gradually extend upwards, and several new cracks are generated on the surface of the concrete slab. The biggest crack in the horizontal range covers the slab width, and the vertical crack area also reaches three-quarters of the slab height. The damage to the concrete slab is the most severe, and the main crack area is trapezoidal (Fig. 8b). From 80% of the ultimate bearing capacity to cessation of loading, stripping concrete, shear keys and steel bar damage occur, as shown in Fig. 8c, which is consistent with Specimen S-2, and the steel bar is subject to significant bending.

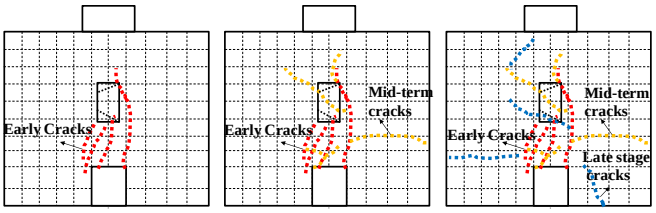

(1) Load: 270 kN (2) Load: 390 kN (3) Displacement: 6 mm

(a) Crack development in Specimen S-4

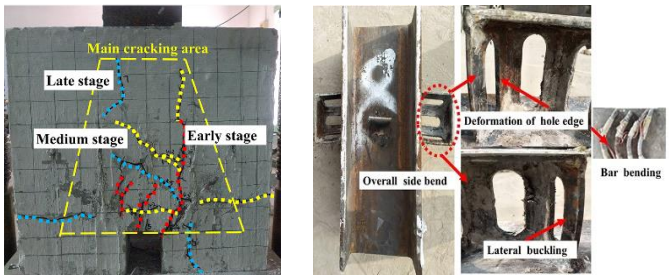

(b) Concrete slab cracks (c) Shear key and steel bar damage

Fig. 8 Destruction of Specimen S-4

S-5 is a stud shear connector; when the load reaches 150 kN, the steel beam slips and cracks appear at the bottom of the stud (Fig. 9b). With increasing load, cracks do not develop rapidly, and no new cracks appear. When the bearing capacity reaches 80% of the ultimate load, cracks appear at the junction of the cast-in-place plate and the prefabricated plate, and oblique cracks appear on the other side of the specimen (Fig. 9c). Under the constraint imposed by the studs, the cracking of concrete slab is slight, and the laminated slab is stratified. Overall, the stud constraint effect is relatively poor, in addition to the point constraint, the integrity of the composite plate is also reduced. Detached concrete and stud failure (Fig. 9e), occurs along with obvious bending along the pushout direction and severe bending in the middle of the web.

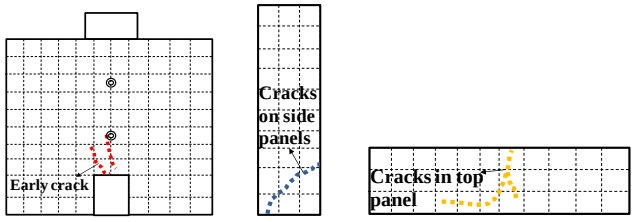

(1) Load: 150 kN (2) Load: 220 kN (3) Load: 240 kN

(a) Crack development in Specimen S-5

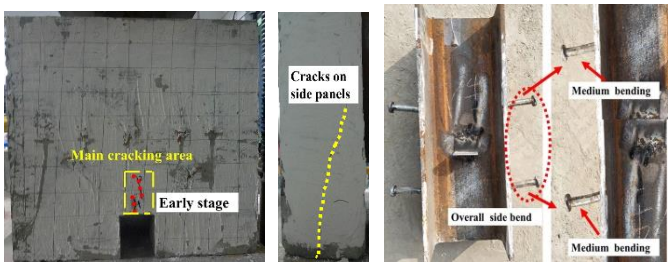

(b) Concrete slab cracks (c) Side cracks (e) Connector damage

Fig. 9 Destruction of Specimen S-5

3.2. Failure mode analysis

Through the push-out tests of five groups of specimens, it is found that the

failure process and mode of concrete slabs are similar; firstly, a 45° oblique crack is formed on both sides of the shear key, subsequently, vertical concrete plate cracks propagate along the shear key. Finally, the trapezoidal main cracking area is formed around the shear key. The top cracking reaches one-third of the plate length, the bottom crack reaches about two-thirds of the plate length, and the height is seven-tenths of the plate height (Fig. 10a). The failure modes of shear keys are similar: along the push-out direction, the steel plate on the outer side of the shear keys buckles, and the edge of the hole edge is slightly damaged, among which the damage in the middle of the hole is the most severely damaged. Compared with double-folded plate shear key, the damage at the opening of triple-folded plate shear key is more obvious, and the overall lateral bending is larger (Fig. 10b). From the analysis of the failure mode, it is found that the rigid shear key failure only occurs in concrete, and the shear key does not deform. The flexible shear key deforms significantly, and then the concrete is damaged under the action of the tensile stress. The flange folded web shear key exhibits semi-rigid characteristics. In the early stage of sliding, the shear bond can work well with the concrete. After sliding, the concrete is damaged, and the shear key undergoes yield deformation, and the failure of both materials occurs synchronously. From the perspective of the failure mode of the new shear key, it can better play the cooperative work performance of steel structure and concrete. On the one hand, it can provide significant stiffness and constrain sliding on the concrete. At the ultimate bearing capacity, it can produce a certain deformation with concrete, allowing adjustment of the internal force. Finally, the better implementation of “constraints” and “deformation” are unified.

In summary, the failure mode and working mechanism of the new shear key and stud are quite different. In the early stage of loading, the shear force is mainly borne by the bond to the concrete. When loaded to the sliding load, the stud is separated from the concrete, and the shear force is mainly borne by the stud. Due to its small stiffness, large deformation occurs at the root in the process of pushing, resulting in local damage to the concrete; because of the stiffness of the stud, the bearing capacity does not decrease. After the opening of the new shear keys, this allows a good bond to the concrete, and the bonding form is changed into mechanical occlusion, and the bearing capacity is greatly improved. Since the web lies at a certain angle, the shear force can be transformed into pressure during the pushing process, which is key to its shear bearing capacity. Another advantage of web oblique layout is that it can reduce the stiffness and increase the deformation capacity. From the perspective of failure mode, the constraint range of studs for concrete is small, showing a point-constraint form, and the shear bond constraint range is larger, showing a trapezoidal distribution. After reaching the ultimate load, the bearing capacity of the shear key decreases, albeit slowly, showing obvious semi-rigid characteristics.

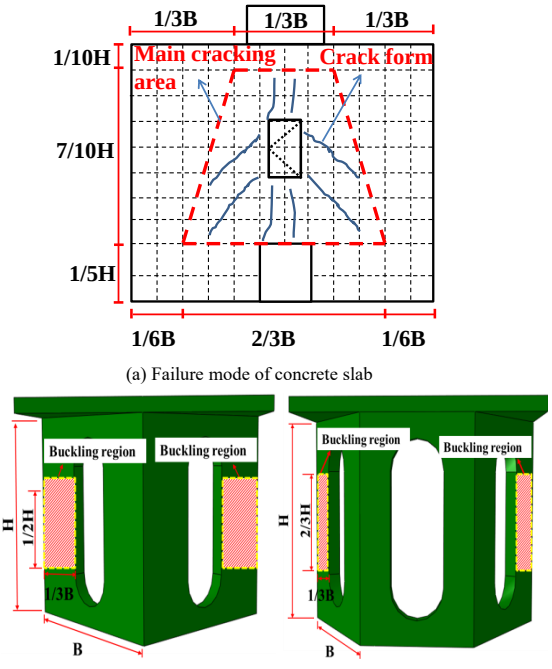

(a) Failure mode of concrete slab

(b) Failure mode of shear key

Fig. 10 Failure mode of a typical specimen

4. Analysis of experimental results

4.1. Load-displacement comparison

The comparison of load-displacement curves of the five groups of specimens is shown in Fig. 11. The failure process is as follows: at the beginning, the bearing capacity increases linearly, and the steel beam does not slip. With increasing load, the steel beam slips and the bearing capacity increases rapidly, while the bearing capacity of the stud increases slowly. After reaching the peak load, the stiffness degrades, the bearing capacity decreases, and the concrete slab is destroyed. The traditional stud shows good deformation ability, and the stiffness and strength degrade slowly. The flange folded web shear key design also exhibits good deformability, and the ultimate bearing capacity and sliding load have been significantly improved. They impose a strong constraint, and provide better integrity, with concrete slabs. Compared with the triple-folded plate shear key design, the double-folded plate shear key has higher ultimate bearing capacity, and the slip load and failure load are similar, indicating that the double-folded plate shear key has good shear performance, and the material strength is fully utilized.

The load-displacement characteristic values of each specimen are illustrated in Table 5, and Fig. 12 depicts the ultimate load and ultimate displacement. Compared with studs, the slip load of the double-folded plate shear key is increased by more than 40 %, and the ultimate bearing capacity is increased by more than 45%. For the triple-folded plate shear key, the sliding load is increased by more than 60%, and the ultimate bearing capacity is increased by more than 30%. The deformation capacity of the two new shear keys reaches more than 61% of the stud. Compared with the triple-folded plate shear key, the ultimate bearing capacity of the double-folded plate shear key is increased by about 11%, and the bearing capacity margin is increased by more than 26%. The double-folded plate shear key and the concrete slab demonstrates better integrity, and the mechanical performance of the shear key is fully developed. Inserting steel bars at the opening has certain effects on the improvement of shear key slip load, deformation capacity, and shear transfer, but the effect is not obvious, which is mainly due to the large difference between steel plate stiffness and steel strength. In summary, compared with studs, the flange folded web shear keys show significantly enhanced bearing capacity, which have a certain deformation capacity. They demonstrate better embedded performance with concrete slabs, and have strong integrity, which can better achieve the design purpose.

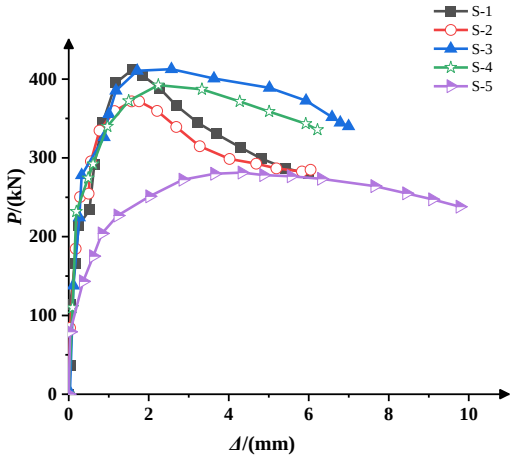

Fig. 11 The comparison of load-displacement curves

Table 5
Eigenvalues of load and displacement

Specimen	Slip load P_y/kN	Ultimate load P_{max}/kN	Displacement of ultimate load Δ_{max}/mm	Failure load P_u/kN	Displacement at failure Δ_u/mm	Bearing capacity margin P_{max}/P_y
S-1	214	412	1.6	280	6.0	1.9
S-2	250	371	1.8	284	6.0	1.5
S-3	277	412	2.2	340	7.0	1.5
S-4	274	392	2.2	335	6.2	1.4
S-5	150	281	4.0	238	9.8	1.9

NOTE: Sliding load P_y is the load corresponding to steel sliding;
Ultimate load P_{max} is the peak load when slipping;
Failure load P_u is the load corresponding to a decrease in peak load to 85 %.

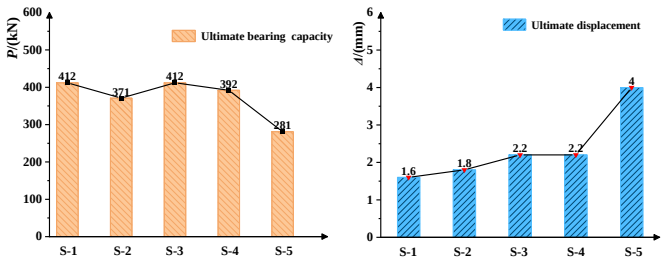

(a) Ultimate bearing capacity (b) Ultimate displacement

Fig. 12 Ultimate load and its corresponding displacement diagram

NOTE: the ultimate displacement is that displacement corresponding to the ultimate load.

4.2. Load-strain analysis

The load-strain relationships of the five groups of specimens are shown in Fig. 13. Flange strain analysis shows that the flange strain of the double-folded plate and the triple-folded plate shear key is small, showing a linear change. Strain analysis in the middle of web openings implies that on the whole, the strain increases with increasing load. Compared with the double-folded plate shear key, the strain in the middle of web openings of the triple-folded plate shear key is larger. A comparative analysis of the left and right-hand folded plate strains shows that the shear key right-hand folded plate (far from the push-out end) strain is less than 10% of left-hand folded plate, in the calculation of bearing capacity, it should be considered as providing a reduction therein. The strain analysis of the inserted steel bar in the hole shows that the strain of the shear key of the inserted steel bar and the uninserted steel bar is the same, and the strain of the shear key of the three-folded plate changes greatly, which is consistent with the failure of the shear key. The strain analysis of the concrete slab indicates that the strain distribution in the concrete slab under the constraint of two new shear keys is more uniform, and the strain therein is larger, indicating that the two new shear keys are better combined with the concrete slab, and the force transmission is more uniform, which agrees with the macroscopic phenomenon found experimentally. Moreover, the concrete under the constraint of the double-folded plate shear key has large ultimate bearing capacity, which fully mobilizes the shear performance of such shear keys.

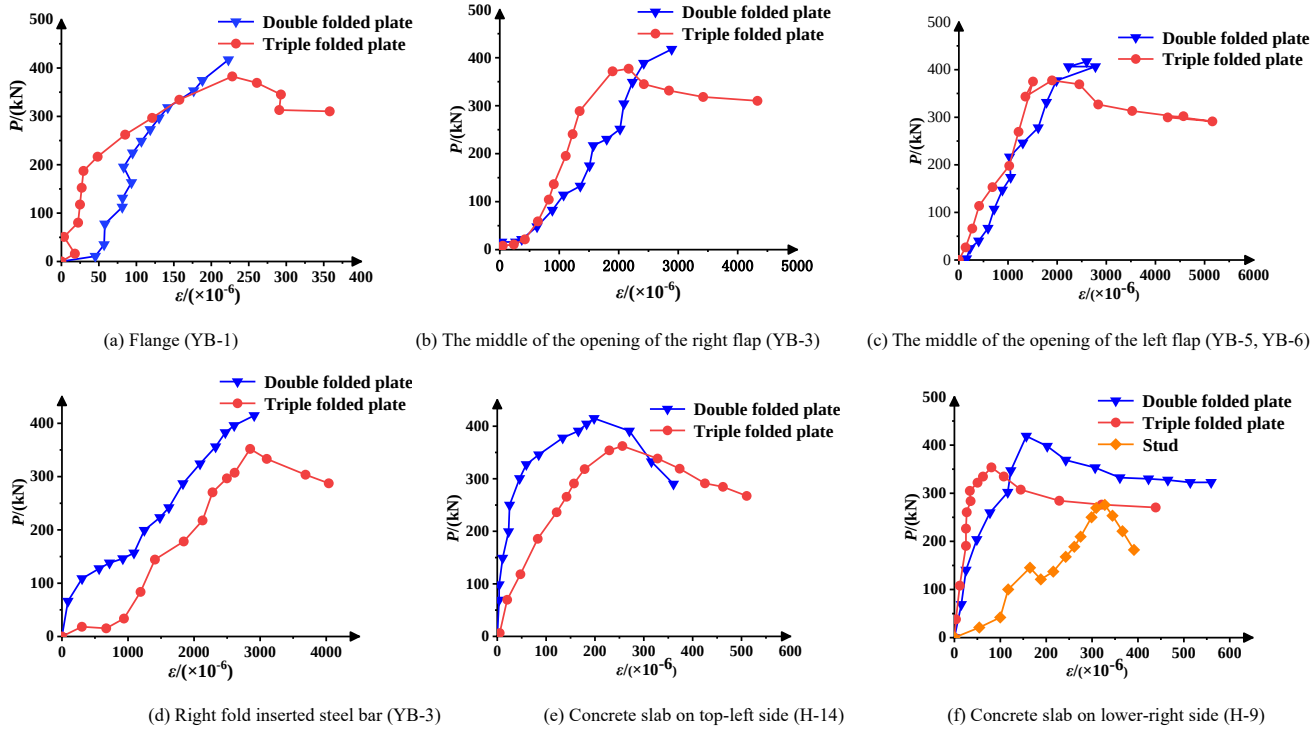

(a) Flange (YB-1) (b) The middle of the opening of the right flap (YB-3) (c) The middle of the opening of the left flap (YB-5, YB-6)

(d) Right fold inserted steel bar (YB-3) (e) Concrete slab on top-left side (H-14) (f) Concrete slab on lower-right side (H-9)

Fig. 13 Comparison of load-strain curves

5. Calculation of bearing capacity and analysis of bond-slip characteristics

5.1. Force model: the shear key

According to the push-out test results and the failure mode of the shear key, the stress on the whole shear key was analyzed. The test pushes the steel beam out along the longitudinal direction of the shear key, the web is subjected to load in two directions (forward and vertical), and the flange is subjected to the same pressure as the push-out direction (Figs. 14a and 14b). On this basis, combined with the test situation, the stress state of each part was simplified and analyzed. The bonding effect between the web and the concrete is negligible when considering the face extrusion between the steel plate and the concrete and the shear effect of the concrete in the hole. The web stress can be divided into three parts: the outer web at the opening, the opening, and the inner web at the opening (corner part); buckling of the lateral web at the opening is the most severe, and the bearing capacity V_1 here mainly depends on the yield strength and the cross-sectional area of the steel plate. The bearing capacity at the opening is V_2. When the specimen is damaged, the concrete in the hole has been destroyed, so the bearing capacity is mainly determined by the compressive strength of the concrete; however, the force distribution is relatively complex here, and the influences of the opening diameter, the angle of the folding plate and the height of the folding plate should be considered at the same time. The bearing capacity of the inner steel plate (corner part) at the opening is V_3, where the stiffness of the steel plate is large, and the bearing capacity is determined by the compressive strength of the concrete. The compressive bearing surface is the transverse projection area of the steel plate. The bearing capacity of flange plate is V_4, which is obtained by the compressive strength of the concrete in the transverse contact part of flange and concrete. According to the strain analysis, the strain in the right-hand steel plate is less than 10% in that in the left-hand steel plate, which is reduced in the calculation of bearing capacity. The triple-folded plate shear key has more intermediate folded plates. Strain analysis shows that the intermediate folded plate strain is small, only considering the shear effect of that concrete in the hole, the bearing capacity is still V_2. The simplified analysis of shear key bearing capacity is shown in Figs. 14c and 14d.

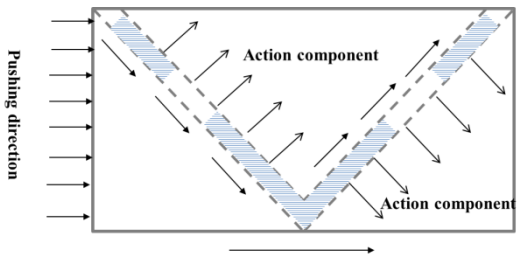

(a) Stress analysis of a shear key in the flange double-folded web

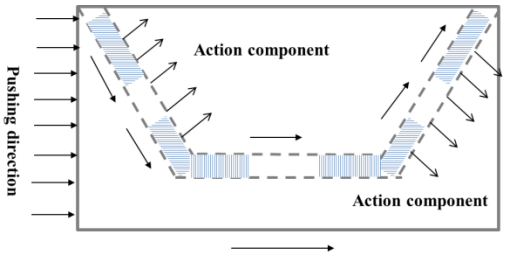

(b) Stress analysis of a shear key in the flange triple-folded web

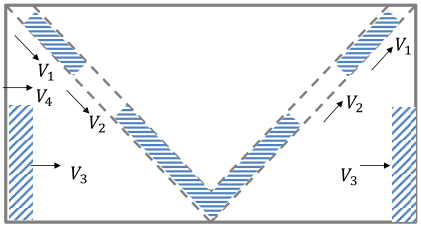

(c) Simplified analysis of the bearing capacity of a shear key in the flange double-folded web

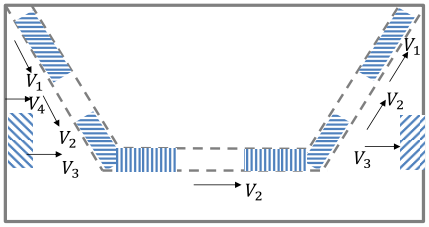

(d) Simplified analysis of the bearing capacity of a shear key in the flange triple-folded web

Fig. 14 Force analysis of a shear key

5.2. Ultimate bearing capacity calculation

Based on the test results, the failure mode of the specimen and the simplified stress model, the calculation formula of the ultimate bearing capacity of the steel plate shear key with the new semi-rigid flange folding web was proposed by considering the factors such as the steel plate strength, the plate height, the hole diameter and the folding angle:

$$V_u = V_1 + V_2 + V_3 + V_4 \tag{1}$$

$$V_1 = b_1 t_1 f_y \alpha_1 \beta \tag{2}$$

where V_u represents ultimate bearing capacity of shear keys; in formula (2), b_1 is width of the plate outside the opening. t_1 denotes web thickness. f_y is yield strength of abdominal plate test. α_1 is the yield strength reduction factor of the whole steel section (usually 0.9). β is the reduction coefficient accounting for the unequal strength of the left and right-hand folded plates (taken as 1.9) according to the difference in strain in the folded plates.

$$V_2 = H_1 t_1 f_{ck} \alpha_2 \beta \cos\theta \tag{3}$$

In formula (3), H_1 is opening height, θ is folding and push-out direction angle and f_{ck} is standard axial compressive strength of concrete. To consider the edge stress concentration strength reduction factor, a value of 0.85 is taken according to engineering experience.

$$V_3 = H b_2 f_{ck} \alpha_3 \beta \sin\theta \tag{4}$$

In formula (4), H represents web height. b_2 denotes the width of the inner web of the opening. α_3 is concrete local compressive strength reduction coefficient, according to engineering experience, a value of 0.9 is taken.

$$V_4 = B t_2 f_{ck} \alpha_2 \tag{5}$$

In formula (5), B represents flange width. t_2 is flange thickness. The comparison between the ultimate bearing capacity values calculated by this formula and the experimental values is displayed in Table 6.

Table 6
Comparison of ultimate bearing capacity between calculated and tested values

Specimen	V_1/kN	V_2/kN	V_3/kN	V_4/kN	V_u	V'_u	Aberration
S-1	78.5	12.95	88.1	8.3	375.7	412	9.7%
S-2	78.5	31.3	88.1	8.3	412.4	371	-10.0%

NOTE: Vu is the theoretical value, and $V'u$ is the experimental value.

By comparison, it is found that the discrepancy between the theoretical calculation value and the experimental value of the ultimate bearing capacity of the two new shear keys is within about 10%. On this basis, the design strength of shear keys was analyzed, as follows:

$$V_k = 0.7 V_u \tag{6}$$

where f_{ck} is the concrete axial compressive design strength f_c, f_y is the designed value of steel strength f.

According to the results of the push-out test, the slip load of the shear key is taken as the actual strength and compared with the theoretical design value (Table 7). The safety margin of a double-folded plate shear key is about 19%, while that of triple-folded plate shear key is more than 60 %. Considering that (P_{max}/P_y) is more than 1.5, it has a high safety factor. This design method can better meet the engineering safety requirements imposed on the shear key.

Table 7
Comparison of design strength and test values

Specimen	Design strength V_k/kN	Test strength P_y/kN	Safety margin
S-1	179.8	214	19.0%
S-2	156.1	250	60.0%

5.3. Analysis of bond-slip characteristics

Herein, a new type of flange folded web shear key was proposed. Its design purpose is to obtain an effective unity of high bearing capacity and deformation capacity, so that it can reflect the semi-rigid characteristics to the fullest extent. In this study, the commonly used rigid shear-T-shaped shear keys (Fig. 15a) and flexible shear-stud (Fig. 15b) in engineering were selected, and the bond-slip characteristics were analyzed with the shear keys with a double-folded web flange (Fig. 15c). The bearing capacity, deformation capacity, and stiffness were compared.

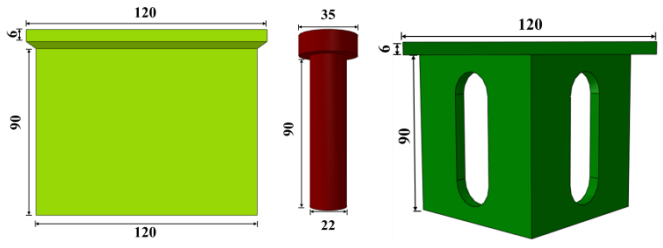

(a) T-shaped shear key (rigidity) (b) Stud (flexible) (c) Flange double-folded web shear key (semi-rigid)

Fig. 15 Form of shear connection

The T-shaped shear key was designed according to the principle of equal geometric size. According to the push-out test of the shear key of double-folded web flange, the dimensions of the T-shaped shear key were obtained as follows: the thickness is 6 mm, the length is 120 mm, and the height is 90 mm. The ultimate bearing capacity of the T-shaped shear key is calculated based on the failure of the left and right-hand sides of the concrete block. The bearing capacity [13] is calculated as follows:

$$P_{uT} = n_2 \eta \alpha_b \alpha_h f_t b h \tag{7}$$

where P_{uT} is the bearing capacity of the T-shaped shear key. b is the thickness of the concrete block. h is the height of concrete block. n_2 represents the number of concrete blocks on both sides of the T-shaped plate ($n_2 = 1$). η denotes the

uniformity coefficient applicable to the left and right-hand sides of the concrete block in terms of the stress thereon (η=1). α_b is the reduction coefficient related to the thickness of the concrete block ($\alpha_{b=1}$). α_h is the reduction coefficient related to the height of the concrete block (α_h =1). f_t is the designed value of the axial tensile strength of the concrete. The bearing capacity of a T-shaped shear key is given by:

$$P_{uT} = n_2\eta\alpha_b\alpha_h f_t bh = 108kN .$$

According to the calculation formula of the bearing capacity of the double-folded plate shear key, the shear bearing capacity is written as:

$$. P_{uy} = 187.85kN$$

The stud was designed according to the principle of equal shear-section area, with a diameter of 22 mm and an overall height of 90 mm. According to the formula for stud bearing capacity proposed in the literature [5]:

$$P_{uS} = 0.29\alpha d^2\sqrt{E_{CM} f_{ck}} / \gamma_v \tag{8}$$

$$P_{uS} = 0.8 f_u(\pi d^2 / 4) / \gamma_v \tag{9}$$

where, P_{uS} is the shear bearing capacity of the stud. E_{cm} is the average elastic modulus of the concrete. f_{ck} is the designed value of the compressive strength of the concrete. f_u represents the tensile strength of the stud material. d is the diameter of the stud.γ_v is the partial coefficient of resistance (γ_v = 1.25, and α = 1). Taking formulae (8) and (9) to calculate the smaller value, the shear bearing capacity of the stud is expressed as:

$$P_{uS} = 0.29\alpha d^2\sqrt{E_{CM} f_{ck}} / \gamma_v = 73.5kN .$$

According to the push-out test on Specimen S-5, the shear bearing capacity of the stud is 70.25 kN, and the error is 4.6%. Formulae (8) and (9) of the stud bearing capacity proposed in the literature [5] are reasonable.

According to *Standard for design of steel structures (GB50017-2017)* [45], shear connector stiffness coefficient is:

$$K = N_v^c (N / mm) \tag{10}$$

where N_v^c is the designed value of the shear connector bearing capacity.

The initial stiffness of the shear connector is the secant stiffness of the straight section of the load-slip curve (Fig. 16), thence the stiffness of the shear connector is deduced:

$$K_1 = \frac{P_1}{\Delta_1} \tag{11}$$

$$P_1 = \alpha_1 P_u \tag{12}$$

where P_1 and P_u are the slip bearing capacity and ultimate bearing capacity of T-shaped shear keys, studs, and double-folded plate shear keys. α_1 is the reduction coefficient applied to the bearing capacity: for a T-shaped shear key this is 0.7, for a stud it is 0.77, and for a double-folded plate shear key it is 0.56. Δ_1 is the slip corresponding to the slip bearing capacity P_1. Before the analysis of bond-slip characteristics, the following settings are made: the stiffness of T-shaped shear bond is large, and the slip bearing capacity is close to the ultimate bearing capacity. Assuming that it reaches the ultimate bearing capacity P_u, its displacement $\Delta_{uT} = 0.1$mm , and when it reaches the slip bearing capacity P_1, its displacement $\Delta_T = 0.07$mm . The stiffness of the stud is small, and the displacement $\Delta_{1s} = 1$mm is assumed to reach the sliding bearing capacity P_1. The displacement of the semi-rigid double-folded plate shear key connector is $\Delta_{1y} = 0.5$mm when the sliding bearing capacity P_1 is reached. After calculation, the stiffness of T-shaped shear key is: $K_{1T} = \frac{P_{1T}}{\Delta_T} = 1080$kN/mm , the stiffness of a stud is: $K_{1s} = \frac{P_{1s}}{\Delta_{1s}} = 54$kN/mm , and the stiffness of a double-baffle shear key is: $K_{1y} = \frac{P_{1y}}{\Delta_{1y}} = 232$kN/mm .

The corresponding displacement P_u when shear connectors reach ultimate bearing capacity Δ_u is:

$$\Delta_u = \Delta_1 + \Delta_2 \tag{13}$$

$$\Delta_2 = \frac{P_u - P_1}{\alpha_2 K_1} \tag{14}$$

The stiffness reduction coefficient after sliding is given: Δ_2 is the slip occurring from reaching the slip bearing capacity P_1 to the ultimate bearing capacity P_u . α_2 is the stiffness reduction factor, for a T-shaped shear key it is 1, for a double-folded plate shear key it is 0.43, and for a stud it is 0.1. By calculation, the limit displacement of the T-shaped shear key is $\Delta_{uT} = 0.1$mm , the limit displacement of a double-folded plate shear key is $\Delta_{uy} = 1.4$mm , and that of a stud is $\Delta_{us} = 4.0$mm .

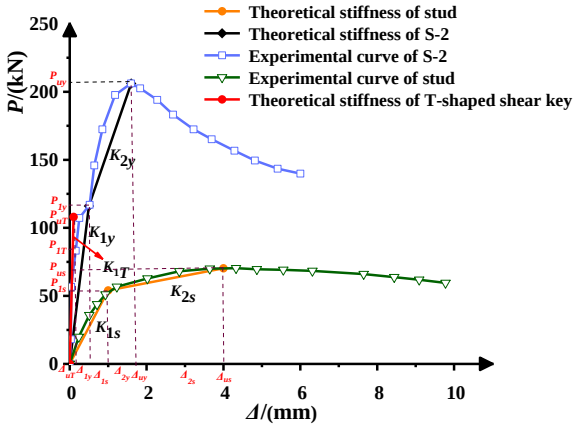

NOTE: P_{1T} , P_{1y} , and P_{1s} denote the sliding bearing capacity of a T-shaped shear key, double-folded plate shear key, and stud;

P_{uT} , P_{uy} , and P_{us} represent the ultimate bearing capacity of a T-shaped shear key, double-folded plate shear key, and stud;

Δ_T , Δ_{1y} , and Δ_{1s} are the displacements corresponding to the sliding bearing capacity P_{1T} of a T-shaped shear key, double-folded plate shear key, and stud;

Δ_{2y} and Δ_{2s} are the displacements generated by the double-folded plate shea r key and the stud from the sliding bearing capacity P_1 to the ultimate bearing ca pacity P_u ;

Δ_{uT} , Δ_{uy} , and Δ_{us} are the displacements corresponding to the ultimate beari ng capacity P_u of a T-shaped shear key, double-folded plate shear key, and stud;

K_{1T} and K_{1s} refer to the initial stiffness of a T-shaped shear key, stud and double-folded plate shear key;

K_{s2} and K_{y2} denote the stiffness after sliding of a T-shaped shear key, st ud, and double-folded shear key.

Fig. 16 Stiffness, bearing capacity, and displacement of a shear connector

The bond-slip characteristics of double-folded plate shear key, T-shaped shear key, and stud were compared (Table 8). Compared with the T-shaped shear key, the slip load of the double-folded plate shear key is increased by 39%, the ultimate bearing capacity is improved by 74%, and the deformation capacity increases more than 10-fold. The ultimate bearing capacity and deformation capacity of the double-folded plate shear key are better than those of the T-shaped shear key. Compared with the stud, the slip load of the double-folded plate shear key is increased by 86%, the ultimate bearing capacity is increased two-fold, and the stiffness is increased almost five-fold. Compared with studs, the initial stiffness and bearing capacity of double-folded plate shear key are greatly improved, which overcomes the problems of low bearing capacity and low stiffness of studs.

In summary, compared with T-shaped shear keys and studs, the ultimate bearing capacity of the double-folded plate shear key has been significantly

improved, which can compensate for the poor deformation ability of the T-shaped shear key and the low bearing capacity of a stud. The stiffness is mobilized between rigid shear connectors and flexible shear connectors, which reflects the obvious semi-rigid characteristics.

Table 8
Comparison of constraint characteristics of a flange double folded web shear key, T-shaped shear key, and stud

Specimen number	Specimen type	Initial stiffness K_1/(kN mm^{-1})	Post-slip stiffness K_2/(kN mm^{-1})	Slip bearing capacity P_1 /(kN)	Ultimate bearing capacity P_u/(kN)	Ultimate displacement Δ_u/(mm)	Initial stiffness ratio	Slip bearing capacity ratio	Ultimate bearing capacity ratio	Limit displacement ratio
1	T-shaped	1080	—	75.6	108	0.1	4.66	0.72	0.57	0.07
2	S-1	232	100	105	187.85	1.4	1	1	1	1
3	Study	54	5.4	56.6	73.5	4.0	0.23	0.54	0.39	2.86

6. Conclusion

In view of the shortcomings of rigid shear keys and flexible shear keys, to obtain the effective unity of high bearing capacity and deformation, the web folding design and hole opening were adopted to improve the bonding effect of the traditional rigid shear bond and concrete, reduce the stiffness, and improve the deformation ability, so as to obtain better performance under load. Through the bond sliding pushing test of the new shear key and the study of force performance analysis and evaluation, the main conclusions are drawn as follows:

(1) Failure mode of a flange folded web shear key: concrete slabs form inclined and vertical trapezoidal main cracking areas, and the range can cover over half of the plate surface. The shear key bends along the push-out direction, and the hole edge undergoes obvious buckling. The new shear key has semi-rigid characteristics. When the concrete is damaged, the shear key also undergoes yield deformation, and the damage to the two materials is quasi-synchronous.

(2) Compared with the stud shear connector, the bearing capacity of flange folded web shear key is increased by more than 40%, and the deformation capacity is increased by more than 60%, showing good bond-slip performance. The effect of inserting steel bars at the opening on the bearing capacity is insignificant.

(3) Strain analysis shows that the strain in the flange folded web shear key is more uniform, the strains are large, and the interaction with the concrete slab is better. The strain in the right-hand folded plate of the shear key (far from the push-out end) is less than 10% of that in the left-hand folded plate, and the reduction is considered in the calculation of the bearing capacity. Based on the shear key stress model, a formula for calculation of the ultimate bearing capacity was proposed, the results from which were in good agreement with the experimental results. The proposed design bearing capacity calculation formula has a high safety margin, which can meet the requirements of engineering application.

(4) The comparison of bond-slip characteristics shows that, compared with the rigid T-shaped shear key, the slip load of the double-folded plate shear key is increased by 39%, the ultimate bearing capacity is increased by 74%, and the deformation capacity increases more 10-fold.

(5) Compared with the flexible stud, the slip bearing capacity of the double-folded plate shear key is increased by 86%, the ultimate bearing capacity is increased nearly two-fold, and the stiffness is increased nearly five-fold, thus fully meeting imposed ductility requirements. The new shear key can overcome the problems of the poor deformation capacity of rigid shear keys and the low bearing capacity of flexible shear keys. It is suggested that the double web form of shear key should be preferred in the future.

References

[1] Ataei A, Zeynalian M."A study on structural performance of deconstructable bolted shear connectors in composite beams", Structures,29 :519-533,2021.DOI: 10.1016/ j.istruc. 2020. 1 1.065.

[2] Zheng S. j, Zhao C, Liu Y.Q, Giovanni Minafò. "Parametric Push-Out Analysis on Perfobond Rib with Headed Stud Mixed Shear Connector", Advances in Civil Engineering, 2019. DOI:10.1155/2019/5952319.

[3] Liu J.P, Zhou B.X , Yu J, Wang Y.H. "Experimental study on the mechanical properties of integral steel-concrete composite beam stud shear connectors", Journal of Building Structures,38 (S1) : 337-341, 2017. DOI:10.14006/j.jzjgxb.2017.S1.047.

[4] Chaves M, Xavier E.M, Sarmanho A, et al. "Study of bolts used as shear connectors in concrete-filled steel tubes", Engineering Structures,231:111697. 2021. DOI: 10.1016 /J. ENGSTRUC T.2020.111697.

[5] D Arévalo, L Hernández, C Gómez, et al. "Structural performance of steel angle shear connectors with different orientation", Case Studies in Construction Materials, 14 (2): e00 523,2021. DOI: 10.1016/J.CSCM.2021.E00523.

[6] Qiu S.Y, Fan J.S, Nie J.G, Tang L, Song S.Y, Xu G.Q. "Shear stiffness test and theoretical study of angle steel connectors", China Journal of Highway and Transport, 34 (03) : 136 – 146, 2021. DOI:10.19721/j.cnki.1001-7372.2021.03.009.

[7] Jiang H.B, Fang H.Z, Liu J, Fang Z.C, Zhang J.F. "Experimental investigation on shear performance of transverse angle shear connectors", Structures,33:2050-2060,2021.DOI: 10.1016/J.ISTRUC.2021.05.071.

[8] Maleki S, Bagheri S. "Behavior of Channel Shear Connectors, Part I:Experimental Study", Steel Construction,64(12):1333-1340,2008. DOI:10.1016/j.jcsr.2008.01.010.

[9] Yan J.B, Hu H.T, Wang T. "Shear behaviour of novel enhanced C-channel connectors in steel-concrete-steel sandwich composite structures", Journal of Constructional Steel Research,166,2020.DOI: 10.1016/j.jcsr.2019.105903.

[10] Vianna J, Costa-Neves L F, Vellasco P, et al. "Structural behaviour of T-Perfobond shear connectors in composite girders: An experimental approach", Engineering Structures,30(9): 2381-2391, 2008. DOI:10.1016/j.engstruct.2008.01.015.

[11] Isabel, Valente, Experimental analysis of Perfobond shear connection between steel and lightweight concrete[J].Journal of Constructional Steel Research,60(3):465-479,2004. DIO:10.1016 /S0143-974X(03)00124-X.

[12] Huang H.L, Bin Z, Zhu M.Q, Zeng C.J, Lv W.R. "Static load push-out test of T-ribbed GFRP shear connectors", Journal of Architecture and Civil Engineering,33 (02) : 77-83, 2016.

[13] Li G.C, Shi X.S, Yang Z.J, Zhang H.E. "Finite element analysis of shear capacity of T-type perforated corrugated plate connectors", Steel Construction,33 (06):6-11, 2018.DOI:1 0.13206/j.gjg201806002.

[14] Yang Y, Chen Y. "Experimental study on shear capacity of PBL shear connectors", Engineering Mechanics,35 (9) : 99-96, 2018.

[15] Mohammed A. Al-shuwaili, Alesssandro Palmeri, Mariateresa Lombardo. "Experimental characterisation of perfobond shear connectors through a new one-sided push-out test", Science Driect Procedia Structural Integrity,13:2024-2029,2018.https://doi.org/10.1016/j. prostr.2018.12.315.

[16] Zhang Y.Z, Li Q, Xia S. "Research on the Influence Factors to the Working Performance of PBL Shear Connectors", Applied Mechanics and Materials,1802,2012.DOI: 10.402 8/ www. scientific.net/AMM.178-181.2192.

[17] João Paulo C. Rodrigues, Luis. Laím. "Experimental investigation on the structural response of T,T-block and T-Perfobond shear connectors at elevated temperatures", Engineering Structures,75(1):299-314,2014.https://doi.org/10.1016/j.engstruct.2014.06.016.

[18] Chen J.B, Wan S, You Y.B. "Experimental study on failure mechanism and bearing capacity of perforated corrugated plate connections", Building Structure, 43 (12) : 74 – 80 + 38, 2013. DOI:10.19701/j.jzjg.2013.12.016.

[19] Yang Y, Yang C. "Experimental Study on Mechanical Behavior of PBL Shear Connectors", Journal of Bridge Engineering,23(9),2018. DOI:10.1061/(ASCE)BE.1943-5592.0001 274.

[20] Yang Y, Yang C, Cai J.W. "Static performance test of perforated steel plate shear connectors", China Journal of Highway and Transport,30 (03) : 255-263, 2017. DOI:10. 197 21/ j.cn ki. 1001-7372.2017.03.028.

[21] Zhu W.Q, Cui Y, Liu Y.J, Heng J.F. "Research on shear capacity of perforated plate connections" Journal of Building Structures,38 (07) : 129-136, 2017. DOI:10.140 06 /j. jzjg xb.2017.07.016.

[22] LF. Costa-Neves, J. P. Figueiredo, P. C. G. da S. Vellasco, et al. "Perforated shear connectors on composite girders under monotonic loading: An experimental approach", Engineering Structures,56(1):721-737,2013. https://doi.org/10.1016/j.engstruct.2013.06.004.

[23] Xue D.Y, Huang Y.C, Wan Q.Y, Zhang Y.D. "Nonlinear analysis of the effect of penetrating steel bars on shear capacity of perforated plate connections", Industrial Construction,50 (11) : 65-70, 2020. DOI:10.13204/j.gyjz201904290005.

[24] Zhang J, Ko L.Y, Hu X.M, Zhang B, Wang C "Experimental study on PBL connectors under long-term load", Industrial Construction,48 (04) :144-152, 2018. DOI:10.1 3204 /j. gyjz20 1804028.

[25] Wang X.W, Zhu B, Cui S.G, Eric M. Lui. "Experimental Research on PBL Connectors Considering the Effects of Concrete Stress State and Other Connection Parameters", Journal of Bridge Engineering,23(1), 2018.DOI: 10.1061/ (ASCE) BE. 1943 – 5592.0001158.

[26] Di J, Zou Y, Qin F.J, Zhou X.H. "Mechanical properties of large-size PBL connectors under strong constraint conditions", China Journal of Highway and Transpor, 31 (03) : 38 – 48 + 58, 2018. DOI:10.19721/j.cnki.1001-7372.2018.03.005.

[27] Zhao C, Liu Y.Q. "Experimental study on shear capacity of perforated plate connectors", Engineering Mechanics,29 (12) : 349-354, 2012.

[28] Shi Q.X, Yang F.Z, Guo J.R. "Study on Bearing Capacity Influence Factors of the PBL Shear Connector", IOP Conference Series: Earth and Environmental Science, 560(1), 2020.DOI: 10.1088/1755-1315/560/1/012038.

[29] Chen H, Guo Z.X, Liu Y, Zheng S.J. "Experimental study on shear performance of PBL shear connector with inclined plate", Journal of Building Structures,43(01):209-218, 2022.DOI:10.14006/j.jzjgxb.2020.0092.

[30] Vetturayasudharsanan Ramasamy,Balaji Govindan. "Feasibility study on triangular perfobond rib shear connectors in composite slab", Materials Today: Proceedings,21 (Pt1): 133-136, 2020.DOI: 10.1016/j.matpr.2019.06.080.

[31] Li Z.X, Wu B, Liao M, Yang X.W, Deng K.L, Zhao C.H. "Experimental investigation on the cyclic performance of perfobond rib shear connectors", Advances in Structural Engineering,23(16):3509-3524, 2020.DOI: 10.1177/1369433220939211.

[32] Suzuki Atsushi, Abe Kanako, Suzuki Kaho, Kimura Yoshihiro. "Cyclic Behavior of Perfobond-Shear Connectors Subjected to Fully Reversed Cyclic Loading", Journal of Structural Engineering,147(3), 2021.DOI:10.1061/(ASCE)ST.1943-541X.0002955.

[33] Zhang Z, Shi J, Li G.Q, Tang Y. "Experimental study on shear capacity of embedded connectors with flanges", Journal of Zhengzhou University (Engineering Science),41 (02) : 86-90, 2020. DOI:10.13705/j.issn.1671-6833.2020.03.008.

[34] Chen J.B, You Y.B, Wan S. "Experimental study on shear behavior of perforated corrugated plate connectors for steel-concrete composite beams", Journal of Building Structures, 34 (04) :

115-123,2013. DOI:10.14006/j.jzjgxb.2013.04.013.
[35] Song R.N, Zhan Y.L, Zhao R.D. “Launch test and numerical analysis of embedded corrugated steel plate shear keys”, China Journal of Highway and Transport,32 (05) : 88-99, 2019. DOI:10.19721/j.cnki.1001-7372.2019.05.009.
[36] Su Q.T, Wang R, Wang W. “Basic mechanical properties test of corrugated perforated plate connectors”, China Journal of Highway and Transport,25 (02) : 46-52, 2012. DOI: 10. 197 2 1/j.cnki.1001-7372.2012.02.007.
[37] Kim Sang-Hyo, Kim Kun-Soo, Lee Do-Hoon, et al. “Analysis of the Shear Behavior of Stubby Y-Type Perfobond Rib Shear Connectors for a Composite Frame Structure”, EngineeringStructures,9(147),114-124,2017.https://doi.org/10.1016/j.engstruct.2017.05.056.
[38] Kun-Soo Kim, Oneil Han, Jonghee Choi, et al. “Hysteretic performance of stubby Y-type perfobond rib shear connectors depending on transverse rebar”,Construction and Building Materials,3(200), 64-79, 2019. https://doi.org/10.1016/j.conbuildmat.2018.12.070.
[39] Sang-Hyo Kim, Oneil Han, Kun-Soo Kim, Jun-Seung Park. “Experimental behavior of double-row Y-type perfobond rib shear connectors”, Journal of Constructional Steel Research,150: 221-229,2018.DOI: 10.1016/j.jcsr.2018.08.012.
[40] Nie J.G, Li Y.X, Tao M.X. “Slip performance and hysteresis model of new pull-out and non-shear connectors”, Engineering Mechanics, 31 (11) : 46 – 52, 2014.
[41] Zhuang D.L, Chen W, Nie X, Duan L.L, Tao M.X, Nie J.G. “Application of non-shear connectors in steel-concrete composite frame structures”, Journal of Building Structures,41 (01) : 104-112, 2020. DOI:10.14006/j.jzjgxb.2018.0503.
[42] Li G.C, Wang Z.Y, Yang Z.J, Xu W. “Experimental study on shear performance of π-shaped perforated plate connectors”, Journal of Building Structures,42 (02) : 131 – 141, 2021. DOI：10.14006/j.jzjgxb.2021.c176.
[43] Zhao X.B, Zhang J.K, Deng W.Q, Liu D, Zhang J.D. “Mechanical performance analysis of dumbbell stud connectors”, World Bridges,48 (06) : 64-69, 2020.
[44] GB/T 10433-2002, “Cheesehead studs for arc stud welding”. Beijing: Standards Press of China,2002.
[45] GB50017-2017, “Standard for design of steel structures”. Beijing: China Architecture & Building Press, 2017.